crystals

MDPI

*Article*

# Impact of Mg on the Feeding Ability of Cast Al–Si7–Mg(0_0.2_0.4_0.6) Alloys

**Mile Djurdjevic [1], Srecko Manasijevic [2], Aleksandra Patarić [3], Srecko Stopic [4,*] and Marija Mihailović [3]**

1 Faculty of Technology and Applied Natural Sciences, University of Applied Sciences Upper Austria, Roseggerstraße 15, 4600 Wels, Austria; miledjurdjevic@yahoo.ca
2 Lola Institute Ltd., 11000 Belgrade, Serbia; srecko.manasijevic@li.rs
3 Institute of Chemistry, Technology and Metallurgy, National Institute of the Republic of Serbia, University of Belgrade, Njegoševa 12, 11000 Belgrade, Serbia; aleksandra.pataric@ihtm.bg.ac.rs (A.P.); marija.mihailovic@ihtm.bg.ac.rs (M.M.)
4 Institute for Process Metallurgy and Metal Recycling, RWTH Aachen University, Intzestrasse 3, 52072 Aachen, Germany
* Correspondence: sstopic@ime-aachen.de

**Abstract:** The demand for high-performance Al–Si casting alloys is driven by their mechanical properties, making them popular in automotive, aerospace, and engineering industries. These alloys, especially hypoeutectic Al–Si–Mg, offer benefits like high fluidity, low thermal expansion, and good corrosion resistance. Silicon and magnesium primarily define their microstructure and mechanical properties. Silicon enhances fluidity, while magnesium improves strength and fatigue resistance. However, challenges like shrinkage porosity persist during solidification. Understanding solidification feeding regions is crucial, influenced by factors such as chemical composition, solidification characteristics, and casting design. This study investigates magnesium's influence on feeding ability in hypoeutectic Al–Si7–Mg alloys through experimental tests. Increasing magnesium content from 0% to 0.6% affects the interdendritic and burst feeding regions. This could impact shrinkage porosity formation. The "Sand Hourglass" test results indicate a rise in porosity levels with higher magnesium content, which is linked to the narrowing of interdendritic channels and the formation of magnesium-rich intermetallic compounds. These changes hinder the liquid metal flow, worsening shrinkage porosity. Therefore, magnesium's role in expanding the interdendritic region is a key factor in developing porosity in cast hypoeutectic Al–Si7–Mg alloys. This study highlights that porosity levels increase from 0% in magnesium-free Al–Si7 to 0.84% in Al–Si7–Mg0.6, underscoring magnesium's significant impact on the occurrence of porosity in these alloys.

**Keywords:** Al–Si7–Mg alloys; magnesium; thermal analysis; feeding effectivity; shrinkage porosity



**Citation:** Djurdjevic, M.; Manasijevic, S.; Patarić, A.; Stopic, S.; Mihailović, M. Impact of Mg on the Feeding Ability of Cast Al–Si7–Mg(0_0.2_0.4_0.6) Alloys. *Crystals* **2024**, *14*, 816. https://doi.org/10.3390/cryst14090816

Academic Editor: Heinz-Günter Brokmeier

Received: 26 August 2024
Revised: 7 September 2024
Accepted: 12 September 2024
Published: 17 September 2024



## 1. Introduction

The popularity of Al–Si casting alloys has resulted in a continuing increase in their demand for components with higher and consistent mechanical properties. The hypoeutectic Al–Si–Mg alloys have widespread applications in automotive, aerospace, and general engineering industries due to their excellent combination of properties such as good fluidity, a low coefficient of thermal expansion, high strength-to-weight ratio, and good corrosion resistance. These foundry alloys possess excellent tensile and fatigue properties and good corrosion resistance. The chemical composition of these alloys significantly impacts all the properties. Two major alloying elements, Si and Mg, in combination with some other minor alloying elements (Sr, Na, Fe, Mn, Ti, B, Zr. . .), outline the metallurgical, mechanical, and structural properties of this alloy [1–4]. Si and Mg are primarily responsible for defining the microstructure and mechanical properties of these aluminum alloys [3–9]. The added amount of Si gives these alloys good fluidity and castability, reducing at the same time shrinkage porosity, while increased Mg improves its strength, hardness, and

fatigue properties [10,11]. However, despite their numerous benefits, Al–Si–Mg alloys face challenges. During the solidification process, various defects may arise, compromising the quality and integrity of the final cast product [12,13]. Among these issues, shrinkage porosity is particularly significant. This defect occurs due to volume contraction during solidification, leading to the formation of cavities or porosity. All aluminum alloys experience a reduction–solidification shrinkage of the volume. The Al–Si hypoeutectic cast alloys shrink by 4–8%, depending on the alloy compositions [5]. During solidification, feeding with liquid melt must compensate for this volume deficit. According to Campbel [7], the solidification of an alloy is divided into five different regions such as: liquid feeding, mass feeding, interdendritic feeding, burst feeding, and solid feeding. Identifying, understanding, and quantifying these feeding regions during the solidification of cast Al–Si7–Mg alloys is essential for implementing effective feeding strategies and optimizing casting quality. Several factors such as chemical composition (Si, Mg, Sr. . .), solidification characteristics (solidification range, intermetallic compound formation), casting design (geometry), casting process parameters (pouring temperature, mold temperature, grain refinement and modification of the aluminum melt), and casting conditions (mold coatings, getting design) influence the feeding ability of cast aluminum alloys [7,14]. Understanding and optimizing these factors are essential for ensuring proper feeding and reducing defects in cast aluminum components. This paper focuses solely on the influence of the major alloying element, Mg, on the feeding ability of hypoeutectic Al–Si7–Mg alloys. Si, the second major alloying element, has been extensively studied in the existing literature, and thus, is not within the scope of this study [1,2,11,15,16]. However, there is a lack of sufficient data in the literature regarding the impact of Mg on various feeding regions. Therefore, this study aims to investigate how variations in Mg's chemical composition (ranging from 0 to 0.6 wt.% in increments of 0.2 wt.%) may affect characteristic solidification temperatures and different feeding ranges of Al–Si7–Mg alloys. This analysis should also provide insights into whether higher levels of added Mg contribute to increased shrinkage porosity in the as-cast structure of these alloys. Several experimental tests were conducted using thermal analysis (TA) and metallographic techniques to achieve this objective.

## 2. Materials and Methods

### *2.1. Materials and Melting Procedure*

The experiments were designed to keep all experimental conditions as constant as possible, except for the alloy composition. This includes known influencing factors, gas and oxide content, and the nucleation state of the melt, as well as uniform, low-turbulence filling of the mold used. Special attention was paid to maintaining low gas content and reproducibly low levels of oxide skins. All melts were free of trace elements (Sr, Na, Sb, Ti, P, B, Pb, Sn . . .) that could affect the characteristic solidification temperatures of these alloys. Pure aluminum (commercial purity 99.7 wt.%), pure silicon (commercial purity 99.9 wt%), and pure magnesium (commercial purity 99.9 wt.%) were used as input materials. All alloys were melted in an electric-resistant 10 kg capacity furnace. No grain refining or modifier agents were added to melts. To determine the influence of the main alloying element, Mg, on the feeding behavior, alloys with their chemical compositions, as shown in Table 1, were used. Their chemical compositions were determined using optical emission spectroscopy (OES) analysis (Type Spectrolab, SPECTRO Analytical Instruments GmbH, Boschstr. 10, 47533 Kleve, Germany).

**Table 1.** Chemical compositions of synthetic AlSi7Mg alloys.

| Alloy | Chemical Compositions (wt. %) | | | | | | |
|---|---|---|---|---|---|---|---|
| | **Si** | **Mg** | **Cu** | **Mn** | **Cr** | **Ni** | **Zn** |
| Al–Si7 | 6.80 | 0.000 | 0.004 | 0.030 | 0.001 | 0.001 | 0.006 |
| Al–Si7–Mg0.2 | 6.92 | 0.202 | 0.007 | 0.004 | 0.002 | 0.002 | 0008 |
| Al–Si7–Mg0.4 | 6.81 | 0.407 | 0.007 | 0.005 | 0.002 | 0.002 | 0.009 |
| Al–Si7–Mg0.6 | 6.81 | 0.590 | 0.006 | 0.004 | 0.002 | 0.001 | 0.008 |

### *2.2. Sand Hourglass Test*

The "Sand Hourglass" technological test, according to Huebler [17], allows for determining feeding behavior under technical conditions. The sample consists of two geometrically identical cylindrical test specimens connected by a feeder neck, as Figure 1 illustrates.

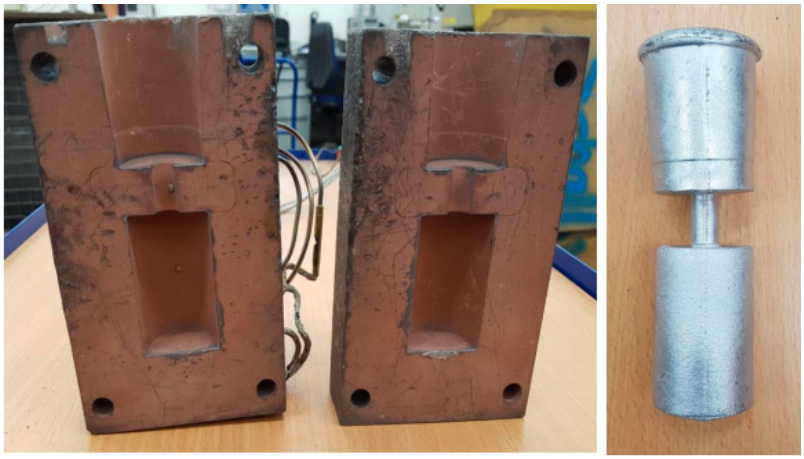

**Figure 1.** "Sand Hourglass" mold (**left**) and sample (**right**).

The upper test specimen acts as a feeder, and the lower test specimen acts as the casting (the volume of each test specimen was approximately 55 $cm^3$, with a mass of about 150 g each). The feeder's neck was dimensioned so the casting was completely fed with optimal feeding capability. With decreasing feeding capability, macro and micro shrinkage pores or defects may form in the casting, depending on the solidification morphology. When the feeder and casting specimens are separated at the center, a standard metallographic procedure can be used to determine the most important feeding mechanical properties. Using the sand hourglass mold, the samples of each alloy listed in Table 1 were cast. The casting temperature was 750 °C, and the mold temperature was 300 °C. The evaluation focused on the lower part of the sand hourglass sample. This part of the sample was again cut in half and ground on a grinding machine with grinding wheels of roughness #80, #320, #500, and #1200. Then, it was photographed for an overview and examined using a stereo microscope (Type: Discovery V20, Carl Zeiss Germany, Carl Zeiss Promenade 10, Jena, Deutschland). Additionally, porosity percentage was determined using an image analysis technique.

### *2.3. Thermal Analysis Procedure*

During all experiments, two TA test samples of approximately 200 ± 10 g each were used to collect the cooling curves of all the investigated alloys from Table 1. Conical steel crucibles with a height of 60 mm and a diameter of 50 mm, weighing 50 g each, were used. Two K-type calibrated thermocouples were also applied, positioned 20 mm above the crucible's bottom, near the wall and at the center of the test cup. Temperature over time was recorded between 700 °C and 400 °C. The thermocouples had an accuracy of ±0.10 °C. The TA data were collected using a high-speed National Instrument data

acquisition system (NI cDAQ-9171) (Type NI cDAQ-9171, National Instrument, 11500 N. Mopac Expwy, Austin, TX, USA) connected to a personal computer. During all trials, the acquisition system recorded five data points (temperature/time) per second. The cooling conditions were constant across all experiments, maintaining an average cooling rate of approximately 10 °C/min for all cooling curves. The cooling rate was calculated as the ratio of the temperature difference between the liquidus and solidus temperatures to the total solidification time within this temperature range.

## 3. Results and Discussions

The predominant and significant issue found in aluminum castings is porosity, stemming from insufficient feeding and/or hydrogen precipitation during solidification. These defects lead to expensive scrap loss and restrict the application of castings in crucial, high-strength scenarios. This study aims to quantify the impact of alloying elements, particularly magnesium, on the characteristic solidification temperatures and different feeding regions. Characteristic solidification temperatures have been determined from the cooling curve analysis. Figure 2 illustrates the impact of various Mg contents on the solidification paths of investigated Al–Si7–Mg(0; 0.2, 0.4, and 0.6 wt.%) alloys.

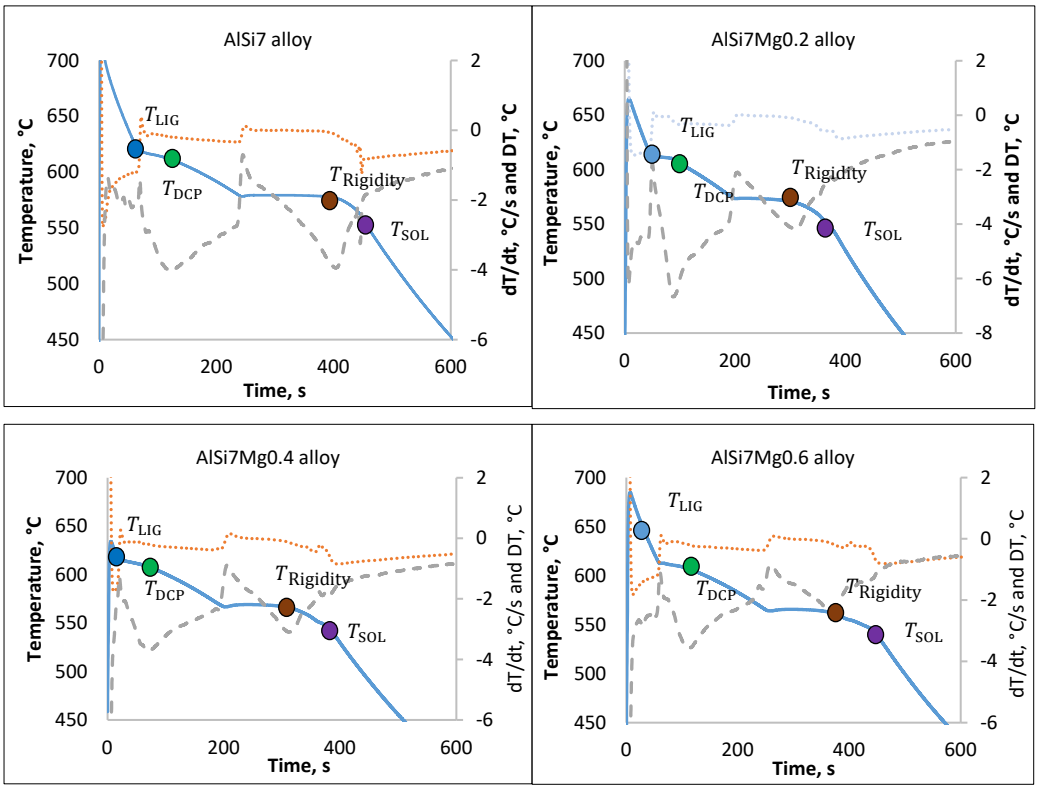


**Figure 2.** Cooling curves of hypoeutectic Al–Si7, Al–Si7–Mg0.2, Al–Si7–Mg0.4, and Al–Si7–Mg0.6 cast alloys.

Figure 2 shows cooling curves (blue solid line), first derivative curves (red dotted line), and ΔT curves (grey dashed line) of hypoeutectic cast alloys Al–Si7, Al–Si7–Mg0.2, Al–Si7–Mg0.4, and Al–Si7–Mg0.6. The dots in Figure 2 indicate characteristic solidification temperatures (liquidus—blue dots, dendrite coherence—green dots, rigidity—brown dots, and solidus—violet dots). As shown in Figure 2, the liquidus and solidus temperatures are determined from the first derivative curves, where the liquidus corresponds to the initial sharp decrease in the cooling rate and the solidus to the almost constant cooling rate at the end of solidification. Dendrite coherency and rigidity temperatures are identified from the ΔT curve, corresponding to the first and second minima, respectively. All these

temperatures, according to Huber et al. [18], were employed to delineate the characteristic feeding regions of the investigated alloys as follows:

- ➢ Liquid feeding: delineated by the pouring temperature and the liquidus temperature.
- ➢ Mass feeding: bordered by the liquidus and dendrite coherency temperatures.
- ➢ Interdendritic feeding: defined between the dendrite coherency and rigidity temperatures.
- ➢ Burst feeding: situated between the rigidity and solidus temperatures.
- ➢ Solid feeding: marked below the solidus temperature.

The impact of various Mg contents on the characteristic solidification temperatures of Al–Si7–Mg alloys has been presented in Figure 3.

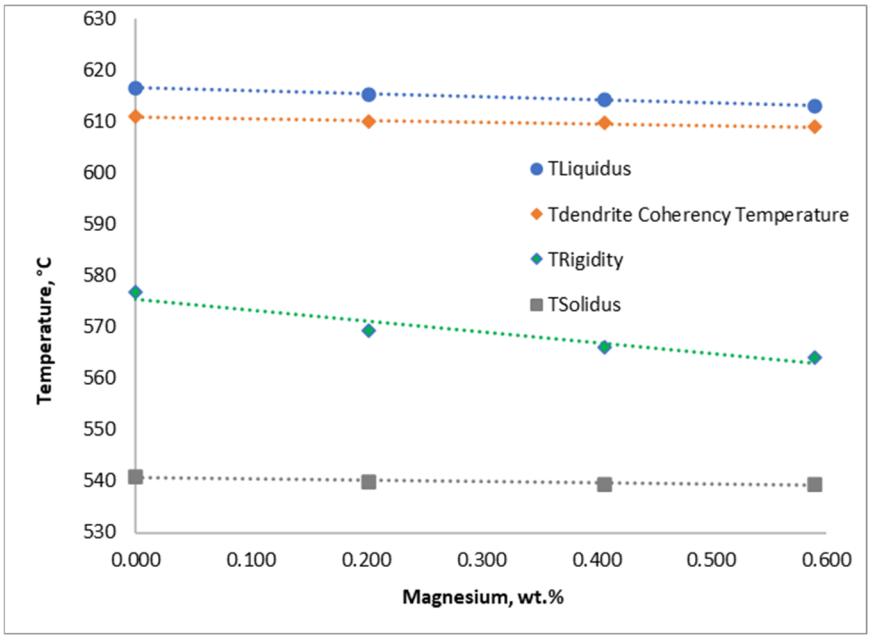


**Figure 3.** Impact of various Mg contents on the characteristic solidification temperatures of Al–Si7–Mg alloys.

Figure 3 shows that any increase in Mg content notably lowered the rigidity temperature and slightly decreased the liquidus and dendrite coherency temperatures, while the solidus temperature was less susceptible to its influence. An increase in Mg content up to 0.6 wt.% led to a decrease in the liquidus temperature by 3.5 °C, the dendrite coherency temperature by 2.2 °C, and the rigidity temperature by 12.7 °C. According to the binary Al–Mg phase diagram, the influence of 0.6 wt.% Mg on reducing the liquidus temperature is evaluated. Derived from this phase diagram, an increase in magnesium content up to the eutectic concentration (approximately 37.9 wt.%) decreases the liquidus temperature to 210 °C. This temperature lowering follows an almost linear trend from 660 °C to 450 °C, corresponding to a reduction of approximately 5.5 °C per 1 wt.% of Mg (or 3.3 °C per 0.6 wt.% Mg). Remarkably, these findings align closely with the results obtained from the cooling curves, which indicate a decrease of 3.5 °C. Drawing on established literature sources [1,19–21], Mg is anticipated to influence the dendrite coherency temperature. It is widely acknowledged that the dendrite size and the solidification cooling rate depend on the concentration of alloying elements present in the melt. During the primary solidification of aluminum alloys, these alloying elements distribute unevenly between the solid and liquid phases. An excess of solute pushed away from the solidification interface into the melt leads to an expansion in the volume of solute situated between already-formed dendrite arms. This state of supersaturation, or its associated constitutional undercooling, serves as the driving force for dendrite growth. Consequently, the space between α-aluminum dendrite arms expands to accommodate the rising concentration of solute elements. Therefore, a higher

concentration of alloying elements, such as Mg, in this instance, induces the precipitation of finer dendrites, thereby lowering their coherency temperature. The presence of Mg in cast hypoeutectic Al–Si7–Mg alloys, according to Figure 3, can lower the rigidity temperature due to the formation of several $Mg_xSi_y$-based precipitates ($Mg_2Si$ being the most common), and the modification of the solidification behavior. The intermetallic phases containing Mg have different melting points than the pure aluminum–silicon eutectic, leading to a shift in the rigidity temperature. Adding Mg to hypoeutectic Al–Si7–Mg cast alloys alters dendritic growth, morphology, and intermetallic phase formation, consequently impacting liquidus, dendrite coherency, and rigidity temperature [1,18]. These changes significantly impact the various feeding ranges, particularly in casting processes where solidification behavior significantly affects the cast components' final microstructure and mechanical properties. The subsequent figures illustrate the influence of different Mg contents on distinct feeding regions: the mass feeding region (Figure 4), the interdendritic feeding region (Figure 5), and the burst feeding region (Figure 6).

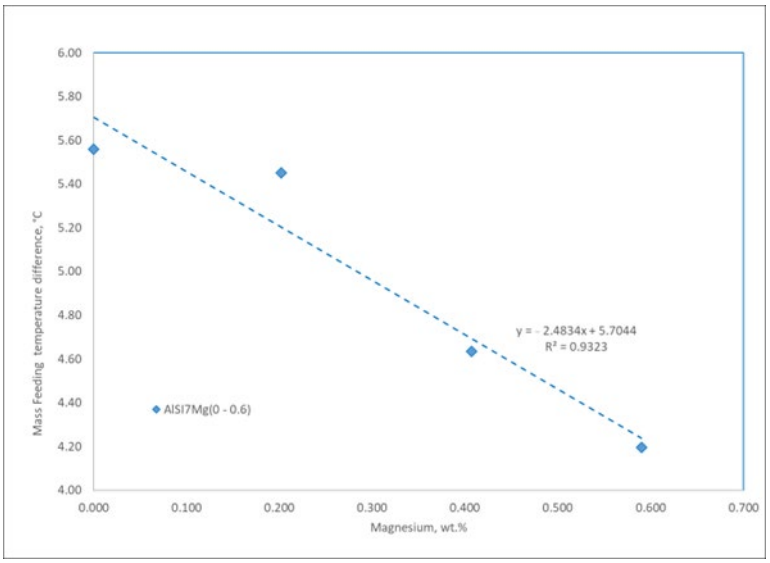


**Figure 4.** Impact of Mg on the mass feeding region of Al–Si7–Mg alloys.

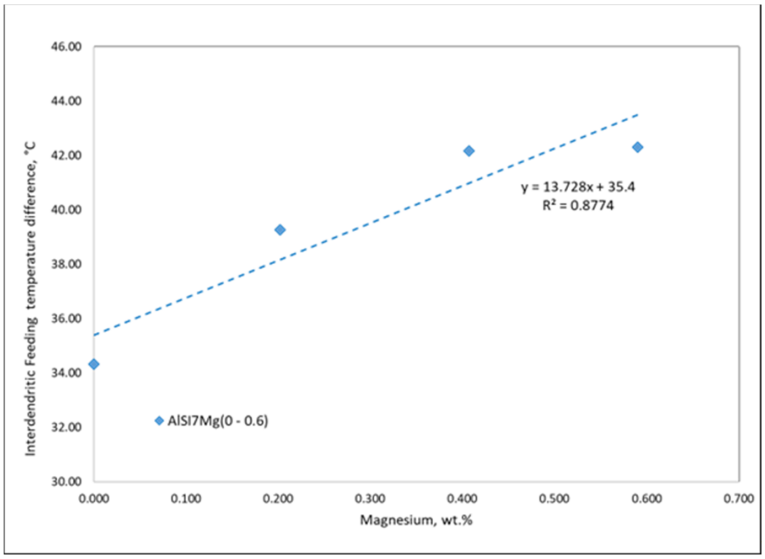


**Figure 5.** Impact of Mg on the interdendritic feeding region of Al–Si7–Mg alloys.

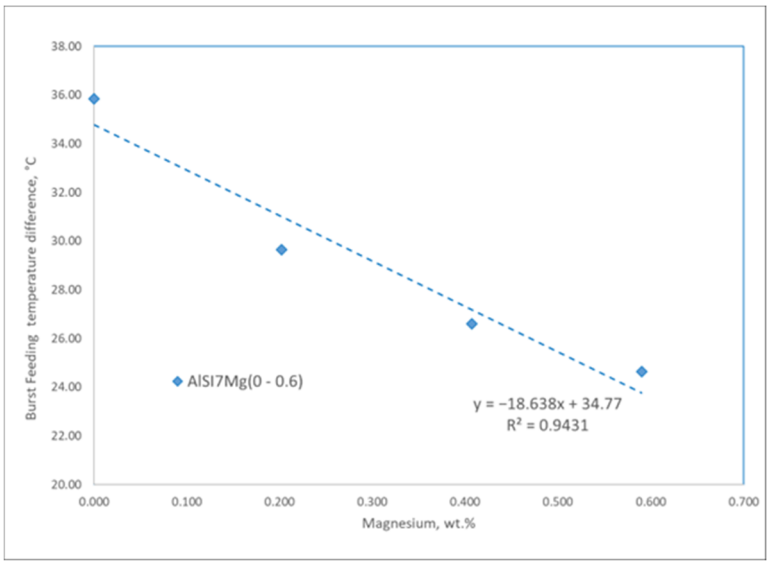


**Figure 6.** Impact of Mg on the burst feeding of Al–Si7–Mg alloys.

As depicted in Figures 4–6, the addition of Mg into Al–Si7 alloys significantly alters the temperature feeding ranges of these alloys. An increased magnesium content decreases the mass and burst temperature feeding range, while a higher Mg content increases the interdendritic feeding temperature range. It has been extensively documented in the available literature that the solidification feeding behavior of cast aluminum alloys is intricately linked to their chemical compositions [15,16,18,22–24]. A study by Cho et al. [22] highlights how adding Mg into Al–Si cast alloys can significantly impact solidification behavior. Michel and Engler [23] observed that adding Mg extends the freezing time, prolongs the eutectic mushy zone, affects feeding ability, and contributes to forming a large amount of micro shrinkage porosity. Dash and Makhlouf [16] further emphasized that, apart from cooling rate, chemical composition also plays a significant role in feeding issues. Their findings suggest that elements such as Fe, Si, Mg, and Cu, present in aluminum alloys during solidification, form various intermetallic compounds such as $Al_5Mg_8Cu_2Si_6$, needle-like $Al_5FeSi$, or $Al_2Cu$. These compounds create a net-like structure that hinders the flow of the melt, leading to the formation of shrinkage porosity. In contrast to previous findings, Sobhan and Chen [24] observed that adding Mg to cast Al–Si alloys reduces the feed demand by narrowing the solidification range. This leads to decreased levels of micro shrinkage and enhances the stability of the alloy.

As depicted in Figure 4, the addition of up to 0.6 wt.% Mg to the Al–Si alloys decreased the temperature range of mass feeding by 1.37 °C. The liquid and mass feedings, which appear at the beginning of the solidification process, are uncomplicated due to a low melt viscosity, wide active feeding path, and relatively elevated melt temperature. The number of dendrites, which start to develop immediately after liquidus temperature, is still not significant enough to slow down the melt movement. Hence, the reduction in the temperature range of mass feeding by 1.37 °C should not significantly affect the feeding ability of these alloys. A significant increase in the temperature range of the interdendritic feeding region of approximately 8 °C, as Figure 5 illustrates, needs to be considered and discussed more thoroughly. This feeding region is delineated with two solidification temperatures: dendrite coherency and rigidity temperature. The crystallization process of aluminum casting alloys initiates with the emergence of primary and secondary $\alpha$-aluminum dendrite networks, originating from a single nucleus. Initially, these nuclei move freely within the liquid melt. As cooling advances, the growing crystals begin to touch each other at the dendrite coherency temperature, forming a cohesive dendrite network. This temperature demarcates the transition between mass and interdendritic feeding regions. Below this threshold, the remaining liquid melt can flow through the

dendrite network but with constraints. A wider interdendritic feeding range signifies a lower melt temperature, higher fraction of solid, increased melt viscosity, and challenging melt feeding ability. An 8 °C increase in the interdendritic temperature range would not be advantageous and could potentially lead to the formation of shrinkage porosity in the as-cast parts. In the interdendritic region, the solid dendritic network maintains permeability. As the melt continues to cool during solidification, the dendrites and their arms grow and expand until the remaining liquid areas within the network lose connectivity, and permeability diminishes. This transition point is termed as the rigidity temperature and marks the boundary between the interdendritic and burst feeding regions. Beyond the rigidity temperature, feeding can only occur through gravity and/or the hydrostatic pressure of the remaining melt, a characteristic feeding method in high-pressure die casting. The observed decrease of approximately 11 °C in the burst temperature range, as illustrated in Figure 6, is expected to enhance the feeding ability of cast Al–Si alloys.

There are only a few papers of the available literature [23,25,26] that attempt, quantitatively, to describe some of the feeding regions of Al–Si alloys. Measuring the time of mass feeding and time of total feeding in the cast parts during solidification, Engler and Michels [23,25] established two criteria that can be used to describe mass feeding and total feeding. The major disadvantage of their approach is that they cannot describe, quantitatively, such feeding regions as interdendritic or burst feeding. Therefore, the foundry industry needs a better quantitative description of those two feeding regions. Recently, to describe the temperature ratio better quantitatively for mass, interdendritic, and burst feedings, the following equations have been proposed [15]:

$$MF = \frac{T_{\mathrm{LIQ}} - T_{\mathrm{DCP}}}{T_{\mathrm{LIQ}} - T_{\mathrm{SOL}}} \times 100 \quad (1)$$

$$IDF = \frac{T_{\mathrm{DCP}} - T_{\mathrm{Rigidity}}}{T_{\mathrm{LIQ}} - T_{\mathrm{SOL}}} \times 100 \quad (2)$$

$$BF = \frac{T_{\mathrm{Rigidity}} - T_{\mathrm{SOL}}}{T_{\mathrm{LIQ}} - T_{\mathrm{SOL}}} \times 100 \quad (3)$$

where:

$MF$, temperature ratio for mass feeding, %.
$IDF$, temperature ratio for interdendritic feeding, %.
$BF$, temperature ratio for burst feeding, %.
$T_{\mathrm{LIQ}}$, liquidus temperature, °C.
$T_{\mathrm{DCP}}$, dendrite coherency temperature, °C.
$T_{\mathrm{Rigidity}}$, rigidity temperature, °C.
$T_{\mathrm{SOL}}$, solidus temperature, °C.

Applying Equations (1)–(3) and calculating the corresponding temperature ratios for various feeding regions, the impact of Mg has been quantified and is presented in Figure 7.

As illustrated in Figure 7, the presence of Mg yields notable effects on both the interdendritic and the burst feeding regions. With an incremental rise in Mg content from 0 wt. % to 0.6 wt. %, the temperature ratio within the interdendritic-constrained feeding areas increases by 15.6%. Conversely, the temperature ratios within the burst feeding regions decrease by approximately 14%. This alteration is visually depicted in Figure 7, where the interdendritic feeding expands, while burst feeding diminishes in duration. These fluctuations in temperature ratios across the interdendritic and burst feeding domains could potentially influence the shrinkage porosity formation in the resultant cast structures.

This study used the "Sand Hourglass" test methodology to investigate how varying Mg additions impact shrinkage porosity formation in several Al–Si7 alloys. By examining the lower portion of sand hourglass samples and employing image analysis techniques to quantify shrinkage porosity, the initial hypothesis is confirmed in Figure 8. The effect of Mg content on porosity in Al–Si7–Mg alloys is shown in Figure 8, accompanied by four sets

of images: macroscopic photographs of test samples and their corresponding processed images used for quantitative porosity analysis. The results illustrate a notable increase in porosity levels, from 0% porosity in the magnesium-free Al–Si7 alloy to 0.84% in the Al–Si7–Mg0.6 alloy, demonstrating the effect of magnesium addition on cast hypoeutectic alloys. The observed increase in porosity can be attributed to the narrowing of interdendritic channels and the formation of precipitated magnesium-reached intermetallics. These factors obstruct the remaining pathways, worsening fluid flow challenges and ultimately leading to the development of shrinkage porosity. Thus, our findings suggest that the expansion of the interdendritic region due to Mg addition serves as the primary driver behind the sensitive occurrence of porosity.

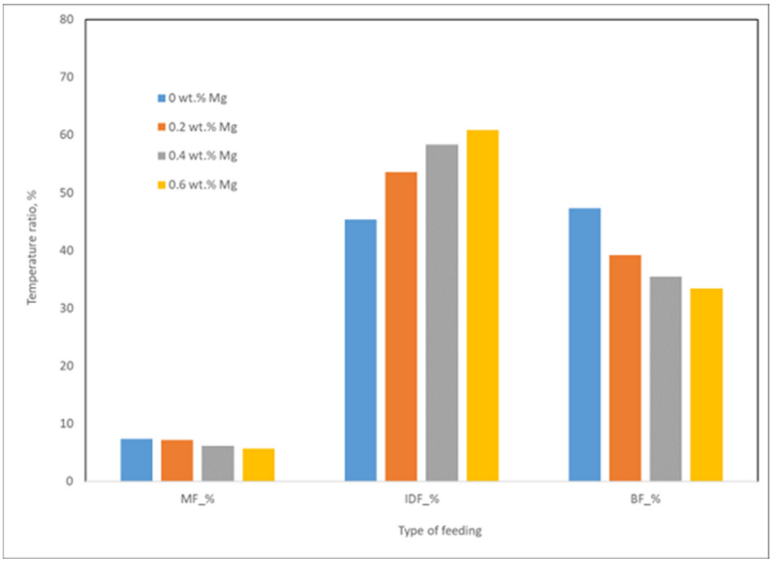


**Figure 7.** The impact of Mg on the temperature ratio of different feeding regions.

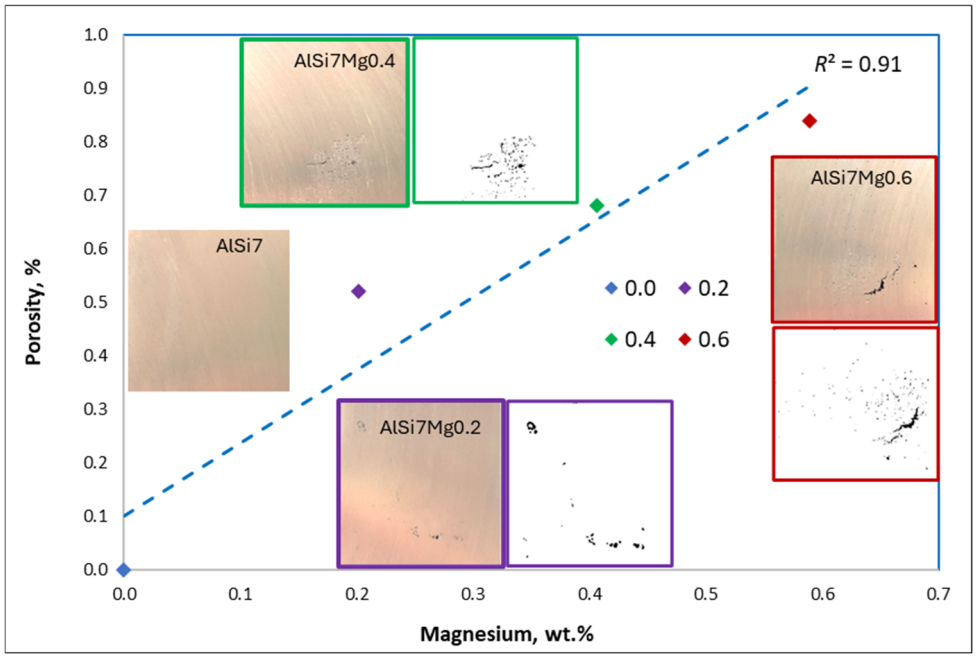


**Figure 8.** Impact of Mg on the porosity of Al–SI7–Mg alloys.

## 4. Conclusions

The impact of Mg on the different feeding regions of Al–Si7–Mg alloys has been studied using the TA technique. It was found that Mg affects the mass, interdendritic,

and burst feeding regions. It can be assumed that the interdendritic-constrained feeding region is more responsible for defect formation by gravity castings, while burst feeding controls the formation of defects by high-pressure die castings. This study reveals a rise in porosity levels, from 0% in magnesium-free Al–Si7 to 0.84% in Al–Si7–Mg0.6, underscoring the impact of Mg in hypoeutectic alloys. This porosity increase is attributed to narrowed interdendritic channels and the formation of magnesium-rich intermetallics. These factors impede the fluid flow, worsening shrinkage porosity development. Therefore, the findings here indicate that the magnesium-induced expansion of the interdendritic region may play a significant role in the occurrence of porosity in cast hypoeutectic Al–Si7–Mg alloys.

**Author Contributions:** M.D.—conceptualization, writing, original draft preparation; S.M.—software application; M.D., S.S. and S.M.—experimental analysis; A.P. and S.S.—literature review; M.M.—writing—review and editing; M.M. and A.P.—visualization and supervision; M.M. and S.M.—project administration. All authors have read and agreed to the published version of the manuscript.

**Funding:** This research received no external funding.

**Data Availability Statement:** The data are unavailable due to privacy.

**Acknowledgments:** This research has been financially supported by the Ministry of Science, Technological Development and Innovation of the Republic of Serbia (Contract No: 451-03-65/2024-3/200066 and 451-03-66/2024-03/200026). The paper was the result of a successful collaboration between researchers from Lola Institute Ltd., Belgrade, Serbia; University of Belgrade—Institute for Chemistry, Technology and Metallurgy—National Institute of the Republic of Serbia; Institute for Process Metallurgy and Metal Recycling, RWTH Aachen University; and University of Applied Sciences Upper Austria.

**Conflicts of Interest:** Srecko Manasijevic was employed by the Lola Institute Ltd., 11000 Belgrade, Serbia. The remaining authors declare that the research was conducted in the absence of any commercial or financial relationships that could be construed as a potential conflict of interest.

## References

1. Callegari, B.; Lima, T.N.; Coelho, R.S. The Influence of Alloying Elements on the Microstructure and Properties of Al-Si-Based Casting Alloys: A Review. *Metals* **2023**, *13*, 1174. [CrossRef]
2. Ervina Efzan, M.N.; Kong, H.J.; Kok, C.K. Review: Effect of Alloying Element on Al–Si Alloys. *Adv. Mater. Res.* **2014**, *845*, 355–359. [CrossRef]
3. Gubicza, J.; Chinh, N.Q.; Horita, Z.; Langdon, T.G. Effect of Mg addition on microstructure and mechanical properties of aluminum. *Mater. Sci. Eng. A* **2004**, *387–389*, 55–59. [CrossRef]
4. Mohamed, A.M.A.; Samuel, F.H.; Alkahtani, S. Bewertung der Wirkung einer Magnesiumzugabe auf der Erstarrungsverhalten von Al-Si-Cu-Gusslegierungen. *Giess. Prax.* **2013**, *7–8*, 286–294.
5. Okorafor, O.E. Some Considerations of the Volume Shrinkage of Aluminium-Silicon Alloy Castings Produced in Full Moulds. *Trans. Jpn. Inst. Met.* **1986**, *27*, 463–468. [CrossRef]
6. Kim, J.M.; Kwon, H.W.; Kim, D.G.; Looper, C.R. Porosity formation in relation to the feeding behavior of AlSi alloys. *AFS Trans.* **1997**, *106*, 825–831.
7. Campbell, J. Feeding Mechanisms in Castings. *AFS Cast. Met. Res. J.* **1969**, *5*, 1–8.
8. Schaffer, P.L.; Lee, Y.C.; Dahle, A.K. The Effect of Aluminum Content and Grain Refinement on Porosity Formation in Mg-Al Alloys. In *Magnesium Technology 2001*; Hryn, J., Ed.; The Minerals, Metals and Materials Society: Warrendale, PA, USA, 2001; pp. 87–94.
9. Arnberg, L.; Dahle, A.; Paradies, C.; Syvertsen, F. Feeding Mechanism in Aluminum Foundry Alloys. *AFS Trans.* **1995**, *115*, 753–759.
10. Di Sabatino, M. On fluidity of aluminium alloys. *Metall. Ital.* **2008**, *100*, 17–22.
11. Di Sabatino, M.; Shankar, S.; Apelian, D.; Arnberg, L. Influence of temperature and alloying elements on fluidity of Al-Si alloys. In Proceedings of the Shape Casting: The John Campbell Symposium, San Francisco, CA, USA, 13–17 February 2005; Tiryakioglu, M., Crepeau, P.N., Eds.; TMS (The Minerals, Metals & Materials Society): San Antonio, TX, USA, 2005; pp. 193–202.
12. Jolly, M.; Katgerman, L. Modelling of defects in aluminium cast products. *Prog. Mater. Sci.* **2022**, *123*, 100824. [CrossRef]
13. Fiorese, E.; Bonollo, F.; Timelli, G.; Arnberg, L.; Gariboldi, E. New classification of defects and imperfection for alluminum alloys castings. *Inter. J. Metalcast.* **2015**, *9*, 55–66. [CrossRef]
14. Di Sabatino, M.; Arnberg, L. Castability of aluminium alloys. *Trans. Indian Inst. Met.* **2010**, *62*, 321–325. [CrossRef]

15. Huber, G.; Djurdjevic, M.; Rafetzeder, M. Impact of Silicon, Magnesium and Strontium on Feeding Ability of AlSiMg Cast Alloys. In *Proceedings of the Materials Science Forum, Thermec 2016*; Sommitsch, C., Ionescu, M., Mishra, B., Kozeschnik, E., Chandra, T., Eds.; Trans Tech Publications Ltd.: Stafa-Zurich, Switzerland, 2016; Volume 879, pp. 784–789.
16. Dash, M.; Makhlouf, M. Effect of key alloying elements on the feeding characteristics of aluminum–silicon casting alloys. *J. Light Met.* **2001**, *1*, 251–265. [CrossRef]
17. Hübler, J. Sanduhrkokille. *Giess. Prax.* **2003**, *95*, 505–512.
18. Huber, G.; Djurdjevic, M.B.; Manasijevic, S. Quantification of feeding regions of hypoeutectic Al–Si (5_7_9 wt.%)–Cu (0–4 wt.%) alloys using cooling curve analysis. In *Mass Production Processes*; Akdogan, A., Vanli, A.S., Eds.; IntechOpen: London, UK, 2019; pp. 1–16.
19. Spear, R.E.; Gardner, G.R. Dendrite Cell Size. *AFS Trans.* **1963**, *71*, 209–215.
20. Gruzleski, J.E. *Microstructure Development During Metal Casting*; American Foundrymen's Society: Des Plaines, IL, USA, 2000; pp. 99–116.
21. Djurdjevic, M.B.; Pavlovic, J.; Byczynski, G. The Impact of Major Alloying Elements and Refiner on the SDAS of Al–Si–Cu Alloy. *Prakt. Metallogr.* **2009**, *46*, 97–114. [CrossRef]
22. Cho, J.I.; Jeong, C.Y.; Kim, Y.C.; Choi, S.W.; Kang, C.S. The Effect of Copper on Feeding Characteristics of Aluminum Casting Alloys. In Proceedings of the 12th International Conference on Aluminum Alloys, Yokohama, Japan, 5–9 September 2010; pp. 745–750.
23. Michel, W.; Engler, S. Speisungskinetik von Aluminum-Silizium Gußlegierungen. *Giesserei* **1988**, *75*, 445–448.
24. Sobhan, S.; Chen, D. A Review on Processing–Microstructure–Property Relationships of Al–Si Alloys: Recent Advances in Deformation Behavior. *Metals* **2023**, *13*, 609. [CrossRef]
25. Michel, W.; Engler, S. Erstarrungsmorphologie und Speisungsablauf von Aluminium- Silizium Legierungen bei Kokillenguß. *Giesserei* **1990**, *77*, 79–82.
26. Pucher, P.; Böttcher, H.; Hübler, J.; Kaufmann, H.; Antrekowisch, H.; Uggowitzer, P. Einfluss der Legierungszusammensetzung auf das Speisungsverhalten der Recyclinglegierung A226 (AlSi9Cu3) im Sand und Kokillenguss. *Giesserei* **2011**, *98*, 34–44.